Life Sciences 91 (2012) 562–571

Contents lists available at SciVerse ScienceDirect

Life Sciences

journal homepage: www.elsevier.com/locate/lifescie

ETS-dependent p16^{INK4a} and p21$^{waf1/cip1}$ gene expression upon endothelin-1 stimulation in malignant versus and non-malignant proximal tubule cells

M. von Brandenstein [a,1], M. Schlosser [a,1], C. Richter [a], R. Depping [b], J.W.U. Fries [a,*]

[a] Department of Pathology, University Hospital Cologne, Cologne, Germany
[b] Department of Physiology, University of Luebeck, Luebeck, Germany

ARTICLE INFO

Article history:
Received 27 October 2011
Accepted 3 April 2012

Keywords:
p16^{INK4a}
p21$^{waf1/cip1}$
ETS
Endothelin-1
Caki-1
RPTEC
Signaling
Receptor

ABSTRACT

Aim: Cellular senescence, leading to cell death through prevention of regular cell renewal, is associated with the upregulation of the tumor suppressor gene p16^{INK4a}. While this mechanism has been described as leading to progressive nephron loss, p16^{INK4a} upregulation in renal cell carcinoma has been linked to a disease-specific improved patient survival rate. While in both conditions endothelin-1 is also upregulated, the signaling pathway connecting ET-1 to p16^{INK4a} has not been characterized until this study.
Main methods: Cell culture, qRT-PCR, Western Blot, immunoprecipitation (IP), proximity ligation assay (PLA), and non-radioactive electrophoretic mobility shift assay (EMSA).
Key findings: In malignant renal proximal tumor cells (Caki-1), an activation of p16^{INK4a} and p21$^{waf1/cip1}$ was observed. An increased expression of E-26 transformation-specific (ETS) transcription factors was detectable. Using specific antibodies, a complex formation between ETS1 and extracellular signal-regulated kinase-2 (ERK2) was shown. A further complex partner was Mxi2. EMSA with supershift analysis for ETS1 and Mxi2 indicated the involvement of both factors in the protein–DNA interaction. After specifically blocking the endothelin receptors, ETS1 expression was significantly downregulated. However, the endothelin B receptor dependent downregulation was stronger than that of the A receptor. In contrast, primary proximal tubule cells showed a nuclear decrease after ET-1 stimulation. This indicates that other ETS members may be involved in the observed p16^{INK4a} upregulation (as described in the literature).
Significance: ETS1, ERK2 and Mxi2 are important complex partners initiating increased p16^{INK4a} and p21w$^{af1/cip1}$ activation in renal tumor cells.

Introduction

Cellular senescence is an aging mechanism that prevents cell renewal leading to apoptosis, and increased expression of the tumor suppressor gene p16^{INK4a} (Verzola et al., 2008). The target p16^{INK4a} functions as an inhibitor of cyclin dependent kinases 4 and 6, which are responsible for the initiation of phosphorylation of the retinoblastoma protein, pRb. This defines the function of p16^{INK4a} as a tumor suppressor gene, interfering with common cell cycle arrest and apoptosis. Its overexpression or loss of function is commonly related to oncogenesis (Hui et al., 2000; Krimpenfort et al., 2001) such as in renal cell carcinoma (Maruschke et al., 2011). In RCC, its expression indicates a better disease-specific survival rate (Ikuerowo et al., 2007). Upon deregulation of gene expression, cell cycle arrest and apoptosis can no longer be properly regulated. In 2001, Ohtani et al. demonstrated that E-26 transformation-specific (ETS) transcription factor family members are able to activate p16^{INK4a} promoter via an ETS-binding site in fibroblasts (Ohtani et al., 2001).

Besides the p16-Rb pathway, senescence is also controlled by the p53-p21$^{waf1/cip1}$ pathway (Jung et al., 2010). The p21$^{waf1/cip1}$ gene, localized on chromosome 6p21.2, produces a smaller 132 amino acid protein due to alternative promoters and splicing. It has been found to induce premature senescence in both normal and tumor cells (Lin et al., 1998) in a p53-dependent manner. It is also elevated in prematurely senescent fibroblasts from human or mice with premature aging syndromes. In the kidney, Ortmann et al. (2004) observed that an improvement of structural injury in glomeruli and podocytes was accompanied by a reduction of the expression of p21$^{waf1/cip1}$. In renal tumor cells (Caki-1) p21$^{waf1/cip1}$ upregulation has been described as pro-apoptotic mechanism targeted by different reagents such as monensin (Park et al., 2003), phenylacetate (Franco et al., 2003), and interleukin-4 (Yu et al., 2004). Gene regulation of p21$^{waf1/cip1}$ is mediated by the direct binding of p53 to two highly conserved p53-response elements. Several other

* Corresponding author at: Institute of Pathology, University Hospital of Cologne, Kerpenerstraße 62, 50924 Cologne, Germany. Tel.: +49 221 478 6061; fax: +49 221 478 6360.
E-mail address: jochen.fries@uni-koeln.de (J.W.U. Fries).
[1] Equal contribution.

0024-3205
doi:10.1016/j.lfs.2012.04.014

transcription factors can activate $p21^{waf1/cip1}$, among others Sp1/Sp3 and E-boxes (reviewed in Jung et al., 2010). In 2003, Zhang et al. described ETS-1 transcriptional activation of $p21^{waf1/cip1}$ as protective mechanism in vascular smooth muscle cells from undergoing apoptosis.

ETS is an evolutionally recent class of transcription factors; among these are ETS-1, ETS-2, Elk1 and GABPα. In the kidney, different ETS proteins have been reported as being upregulated and having greater impact than other family members, such as ETS1 and 2 (Hollenhorst et al., 2004). All ETS proteins have a highly conserved, helix-turn-helix core consensus sequence as DNA binding domain with a central 5-GGA(A-T)-3 core motif (Jedlicka and Gutierrez-Hartmann, 2008). ETS proteins are important in the regulation of: proliferation, migration, differentiation and apoptosis; but upregulation or increased amplification can be as well associated with oncogenesis (Gutierrez-Hartmann et al., 2007; Puri et al., 2006). An important molecular feature regulating the transcription of genes is the pointed domain (PNT). The PNT of ETS1 contains an extracellular signal-regulated kinase 2 (ERK2) docking site that enhances the phosphorylation of a mitogen-activated protein kinase (MAPK) site, N-terminal to the PNT domain (Seidel and Graves, 2002).

MAPKs are cytoplasmic serine/threonine kinases, activated by extracellular stimuli such as: cell proliferation, differentiation, and inflammation. Various isoforms and splicing variants have been identified for p38α. Among them, Mxi2 is identical to p38α in the first 280 amino acids, harboring a unique 17 amino acid C-terminus (Zervos et al., 1995). Mxi2 is most abundant in renal tissues (Faccio et al., 2000), can bind to ERK1/2 and regulates its nuclear transport (Sanz-Moreno et al., 2003).

Endothelin-1 plays a major role as mediator of cellular signaling in primary renal proximal tubule cells (Ong et al., 1995) and their malignant counterparts from renal cell carcinoma, Caki-1 cells (von Brandenstein et al., 2008). This signal transmission is mediated via the Endothelin A (ETA) receptor, present in both human cell types (Gerstung et al., 2007; von Brandenstein et al., 2011). In this context, we demonstrated an ET-receptor dependent, protein–protein interaction between: nuclear factor-kappa B (NF-κB) p65, mitogen-activated protein kinase (MAPK) p38 and protein kinase C alpha (PKCα) as part of the transcription complex (von Brandenstein et al., 2008, 2011). Since ETS and Mxi2 are present in the kidney, and ERK may be upregulated after endothelin-1 stimulation via the ETA receptor (Chen et al., 2009), these factors seemed likely candidates for a significant role in $p16^{INK4a}$ activation. In this study we investigated whether endothelin-1 and its two ET-receptors are involved in the signaling function via ETS, Mxi2 and MAPK transcription to regulate $p16^{INK4a}$ activation in human renal carcinoma and normal proximal tubule cells.

Materials and methods

All reagents used were commercially available at Sigma-Aldrich, except when otherwise specified. All experiments were performed in triplicates, except when otherwise specified.

Blobfinder

For quantification of the Eurogentec experiment the free commercial software, Blobfinder, was used according to the manufacturer's recommendation (http://www.cb.uu.se/~amin/BlobFinder/). To quantify differences not readily visible by microscopic inspection, this program can help by analyzing the images based on a single cell analysis. This analysis simulates cytoplasm and assigns each signal to a particular cell. In the output, every cell has a value representing the number of signals in that particular cell compartment.

Cell culture

Caki-1 (renal cell carcinoma cell line) and RPTEC (primary renal proximal tubule epithelial cell line) cells were cultured as previously described (Gerstung et al., 2007; von Brandenstein et al., 2008, 2011).

Cell treatments

Cells were treated with endothelin-1 (50 nM) for different time points. Before treatments the cells were serum starved for 24 h. Endothelin A and B receptor blocks were done as previously described (Gerstung et al., 2007).

Densitometry

For densitometric analysis the ImageJ program was used according to the protocols. A measuring area was placed around the individual signal and its intensity was measured. The same area was then used to measure the background signal (noise) of the respective Western blot. The two values were subtracted from each other. The same procedure was followed for all signals and their respective Western blot "noise." To determine the net signal of each band, the corresponding calculated value of the β-actin loading was regarded as 100%, and the proportional value of each of the protein signals was calculated.

The same procedure was followed analyzing the EMSAs including the supershift. After the signal-to-noise ratio was calculated, the untreated control Caki-1 cells were regarded as 100% and squared with the ET-1 treated ones. The two supershift bands were equally squared with their untreated controls.

Immunoprecipitation

For immunoprecipitation, either ETS1, ERK2 or Mxi2 agarose conjugated antibody (Santa Cruz) was used. The assay was performed according to the Santa Cruz protocol with 1000 μg total cellular protein. The final washing step was done 3× with PBS and the samples were diluted in 5 μl 2× electrophoresis sample buffer. After a boiling step of 4 min, the samples were centrifuged and used for Western blot analysis.

Non-radioactive electrophoretic mobility shift assay (EMSA)

Nuclear extracts were isolated from endothelin treated and untreated cells according to the manufacturer's protocol (Nuclear extraction kit, Active motif). Protein content was assayed with the Bradford protein assay (Bio-Rad) with BSA as standard. Double stranded $p16^{INK4a}$ oligonucleotides (Alexa 660 TTC CGC CAG CAC CGG AGG AAG AAA GA) were commercially synthesized (Invitrogen) and the forward strand was labeled with Alexa 660. $p16^{INK4a}$ binding reactions were conducted in 200 mM TRIS–HCL pH 7.6, 50 mM $MgCl_2$, 0.1 mM EDTA and 10 mM DTT. To prepare the DNA for annealing, the oligonucleotides (1.5 nmol each) were incubated at 70 °C for exactly 10 min and a further 30 min at room temperature. For the protein/DNA binding reaction, 20 μg of protein was added to the samples and incubated on ice for 30 min. The reaction was analyzed by electrophoresis in a non-denaturation 6% polyacrylamide gel in 1× TBE buffer. For supershift EMSAs, ETS1 or Mxi2 antibody (Santa Cruz) was used. As negative control, 200× more concentrated non-labeled, "cold" $p16^{INK4a}$ oligonucleotide was incubated with 20 μg of protein and added to the Alexa labeled sample. As a binding and negative control, a mutated $p16^{INK4a}$ (Alexa 660 CTT CCG CCA GCA CCG GCT TCC TAA AGA, Invitrogen) oligo was used. All EMSAs were performed in triplicates and visualized with a fluorescence reader (Licor, Licor Biosciences).

For $p21^{waf1/cip1}$ the following oligonucleotides were used (Cy5 AGG TCA GCT GCG TTA GAG GAA GAC T) (Zhang et al., 2003), the mutated oligonucleotide (Cy5 AGG TCA GCT GCG TTA GAT CCG AAG ACT), the corresponding reverse strand was unlabelled. The $p21^{waf1/cip1}$ oligos were synthesized by eurofins mwg operon. The EMSA was performed as mentioned above; the running time was 120 min.

Nuclear extract and cytoplasmic isolation

Nuclear and cytoplasmic extracts were isolated from treated cells and controls according to the manufacturer's protocol (nuclear extraction kit, Active motif). Protein content was assayed with the Bradford protein assay (Bio-Rad) with bovine serum albumin as standard.

Proximity ligation assay by Duolink kit

1×10^4 Caki-1 cells grown on Labtecs were washed with PBS and incubated according to the manufacturer's protocol (OLink Bioscience). The mixture was incubated in DMEM at room temperature for 15 min. DMEM was removed; the cells were washed with PBS and treated with 50 nm ET-1 for 24 h. For fixation, a methanol:acetone (1:1, v/v) mixture was used. After removal of DMEM, slides were washed in PBS, air dried, and incubated in ice-cold methanol:acetone (1:1, v/v) for 90 s. After the fixation procedure, the Duolink kit was used according to the manufacturer's instructions. The cells were incubated with a blocking solution in a pre-heated humidity chamber at 37 °C for 30 min, followed by primary antibody incubation for 2 h at room temperature. Incubation with the PLA probes for 1.5 h at 37 °C followed, and the detection protocol; according to the recommended time points; was applied. After completing the final step, slides were mounted in Invitrogen fluorescence mounting medium with DAPI (Invitrogen) for nuclear staining. The Leica Aristoplan microscope with Discus software was used for visualization.

RNA isolation

RNA was isolated with the RNeasy kit from Qiagen according to the manufacturer's protocol. RNA was quantified using the NanoDrop technology.

RT-PCR

The cDNA was obtained from 250 ng RNA using random primers and SuperScript III reverse transcriptase according to the manufacturer's protocol (Invitrogen). In order to be in the semi-quantitative range, the amount of cDNA was previously determined by titration and the number of PCR cycles was standardized. The PCR reactions were performed in a final volume of 25 µl. For PCR reaction, 1 µl of the RT-PCR product was always used and mixed with RedTaq Ready Mix (Sigma) or Platinum Taq polymerase (Invitrogen) according to the manufacturer's protocol. The PCR reactions were performed with 35 cycles consisting of 0.5–1 min at 94 °C, 1 min at 55 °C annealing temperature, 1 min at 72 °C with a final extension for 10 min at 72 °C.

Primers: β-actin, forward: TTG GCA ATG AGC GGT TCC GCT G, reverse: TAC ACG TGT TTG CGG ATG TCC AC, temperature 55 °C, 35 cycles; ETS1 forward: ACC CAG CCT ATC CAG AAT CC, reverse: TCT GCA AGG TGT CTG TCT GG; ELF-1 forward: TCA AGT CCA GGG GTA AAA GG, reverse: TTC ATC CTG CAT GGT ACT GG, temperature 55 °C, 35 cycles; ELK1 forward: CCA CCT TCA CCA TCC AGT CT, reverse: AAC CCG GCT CCA CAT TAA G, temperature 55 °C, 35 cycles; ESE1-ELF3 forward: GCA ACT ACT TCA GTG CGA TGT AC, reverse: CAG TCC AGA ACC TGC GTC TT, temperature 55 °C, 35 cycles; ES3-EHF forward: GGA AGG AGG TGG TGT AAT GAA TC, reverse CCA CTC CCA CAC CTG GTA CT, temperature 55 °C, 35 cycles; ETS2 forward: CAA GGC TGT GAT GAG TCA AGC, reverse: GGT GCC AGC TCC AGA AAG C, temperature 55 °C, 35 cycles; GABPα forward: CAC CAT GCT GAA TCA GAA GC, reverse: TGC TGA ATT CCT TCA TTA CCC, temperature 55 °C, 35 cycles; MEF-ELF4 forward GCA GCA CCA TCT ATC TGT GG, reverse: ACT GGT ACA CCA GCC TCT GC, temperature 55 °C, 35 cycles; NERF-ELF2 forward: ACC ACT GCA TCT GTG TCA GC, reverse: TGC ATG GTG ATT TTG TCTC C, temperature 55 °C, 35 cycles; NET-ELK3 forward TCC ACT GCT CTC CAG CAT AC, reverse: GGA GAA GCA GCT CTG TGT CCA, temperature 55 °C, 35 cycles; PU.1 forward: CCA CTG GAG GTG TCT GAC G, reverse: GTC ATC TTC TTG CGG TTG C, temperature 55 °C, 35 cycles; SAP1-ELK4 forward: GCA GAA GCC TCA GAA CAA GC, reverse: TTG GAT CCA TGT TCA AAA TCT CTG G, temperature 55 °C, 35 cycles; TEL-ETV6 forward: CCA TCA ACC TCT CTC ATC GG reverse: GGC TCT GGA CAT TTT CTC ATA GG, temperature 55 °C, 35 cycles; TEL-ETV7 forward: AGG GCT TAC CAG CAA CTT CG, reverse: GGG CTC ATA TCG GGT ATC AA, temperature 55 °C, 35 cycles; $p16^{INK4a}$ forward: CTT CCT GGA CAC GCT GGT, reverse: GCA TGG TTA CTG CCT CTG GT, temperature 50 °C, 35 cycles.

Statistics

All experiments were performed in triplicate.

The GraphPrism 5 program was used for performing statistical analysis. After the analysis of variance (one way ANOVA) was performed, significant differences were calculated using mean ± SEM.

Western blot analysis

Western blot analysis was performed as previously described (Gerstung et al., 2007; von Brandenstein et al., 2011, 2008) For the

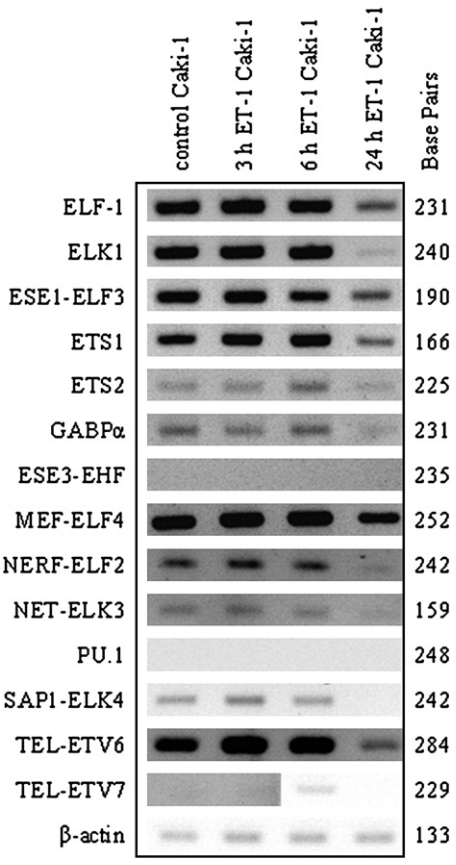

Fig. 1. Expression level of ETS transcription factors in Caki-1 cells. Subconfluent cells were stimulated with 50 nM ET-1 for 3, 6, and 24 h. After RNA extraction, 250 ng was reverse transcribed, and a PCR reaction was performed using primers for ETS transcription factors. PCR products were analyzed on a 2% agarose gel. The experiment, starting from ET-1 treatment of Caki-1 cells, was performed in triplicate.

analysis of the ETS1, GABPα, ETS2, and β-actin antibodies from Santa Cruz were used and tested for specificity with Santa Cruz designed peptides.

Results

Endothelin-1 dependent ETS transcription family members

ETS transcription factor family members were analyzed in triplicate for their expression patterns in Caki-1 cells. To study the influence of time on ET-1 stimulation, cells were treated for 3, 6, and 24 h with 50 nM ET-1 (Fig. 1). The PCR products were analyzed by agarose gel electrophoresis on a 2% agarose gel, run at 120 V. After 24 h ET-1 stimulation a decrease of expression was detectable for all ETS transcription factors. However, ETS1, ETS2 and GABPα showed an increased expression after 6 h ET-1 stimulation. All three transcription factors were analyzed by Western blot. Since ETS1 upregulation was the strongest among these three proteins, it was chosen for further analysis.

Cytoplasmic versus nuclear expression of ETS1 in ET-1 stimulated Caki-1 cells

20 μg protein isolated from the cytoplasmic and nuclear fraction of 50 nM ET-1 stimulated Caki-1 cells was used for Western blot analysis (Fig. 2) ($n=3$). β-actin levels showed equal loading of protein. An increase of nuclear ETS1 was observed after ET-1 stimulation over time, compared to nuclear controls ($p \leq 0.001$). In contrast, after ET-1 stimulation no significant change in ETS1 levels in the cytoplasm could be observed after 24 h treatment (Fig. 2A and B). Fig. 2C and D demonstrates the ETS2 expression over time in the cytoplasmic and nuclear fraction. After ET-1 treatment no migration of ETS2 was detectable.

Endothelin receptor dependent ETS1 expression

After 24 h of serum starvation, Caki-1 cells were either treated with ET-1 for 24 h or the endothelin A or B receptor was specifically blocked 1 h before ET-1 treatment. As shown in Fig. 3A ($n=3$), statistically significant reduction of ETS1 protein levels in the nucleus was detected after either ETA or ETB receptor block. However, the ETS1 reduction was more significant after ETBR block (Fig. 3B).

Analysis of participating proteins in complex formation after ET-1 stimulation

As it was already known that ETS1 presents a docking site for ERK2, immunoprecipitation was done with ETS1 and ERK2 conjugated agarose beads (in triplicate; Fig. 4). 1000 μg total cellular extract was immunoprecipitated from Caki-1 cells stimulated with 50 nM ET-1 for 24 h, followed by Western blot analysis. The setups identified a complex formation between ETS1 and ERK2. The same approach was used to identify the complex formation between ERK2 and Mxi2. To ensure that all three proteins are present in the same complex, immunoprecipitation with ETS1 and Mxi2 conjugated agarose beads was also performed. The results obtained indicated a complex formation between ETS1, ERK2 and Mxi2.

Cellular location of protein complex in Caki-1 cells

To analyze the location of the complex in the cell, duplicate proximity ligation assays were performed (Fig. 5). A complex formation between ETS1 and ERK2 as well as ERK2 and Mxi2 was detected. In both experimental setups all cells were positive for DAPI. The cells showed multiple fluorescent dots in the nucleus, indicating positive signals for the tested complex partners. Pairwise comparison of control cell populations against ET-1 stimulated cell populations revealed

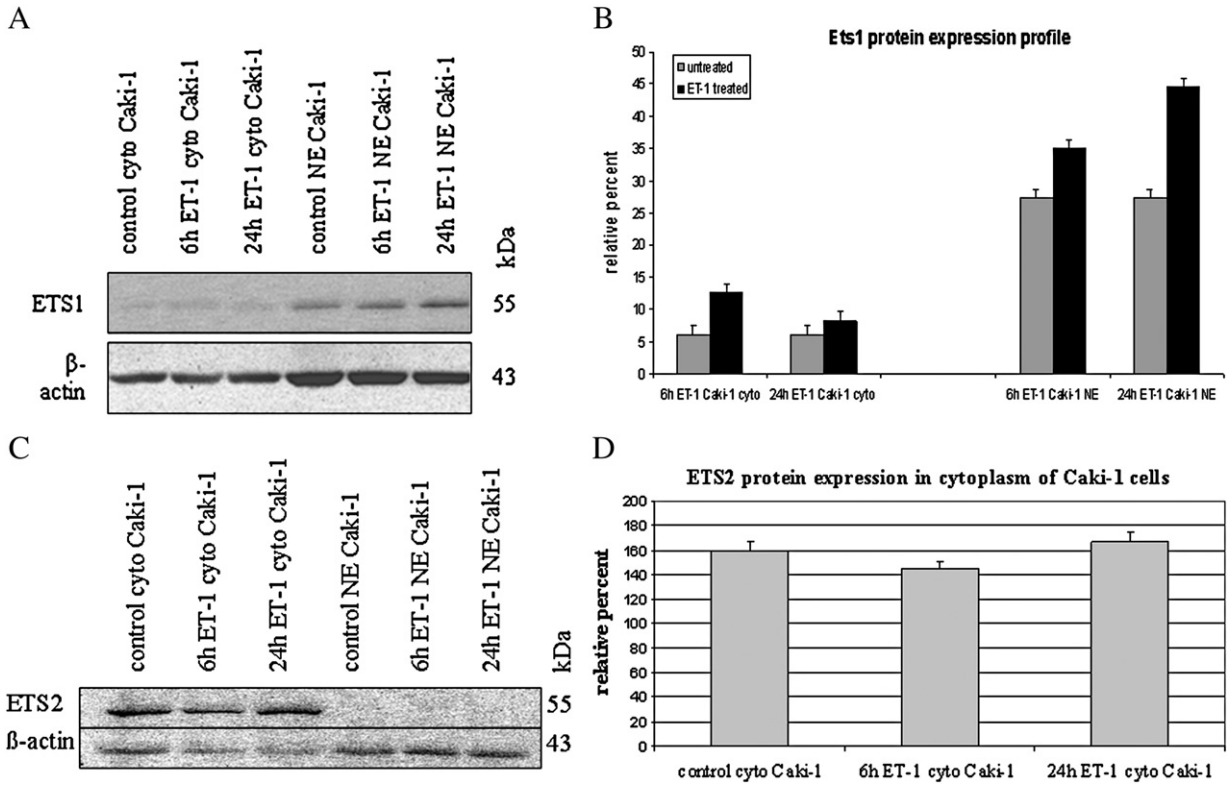

Fig. 2. Western blot analysis was performed in triplicate for ETS transcription factors in Caki-1 cells. In A and C, 20 μg protein from prepared nuclear or cytoplasmic cell extracts after ET-1 stimulation with 50 nM for 6, and 24 h was used. β-actin served as a loading control. In B, densitometric analysis of performed Western blots. In D, densitometric analysis of performed Western blots; changes were not significant. Cyto: cytoplasmic; NE: nuclear extract.

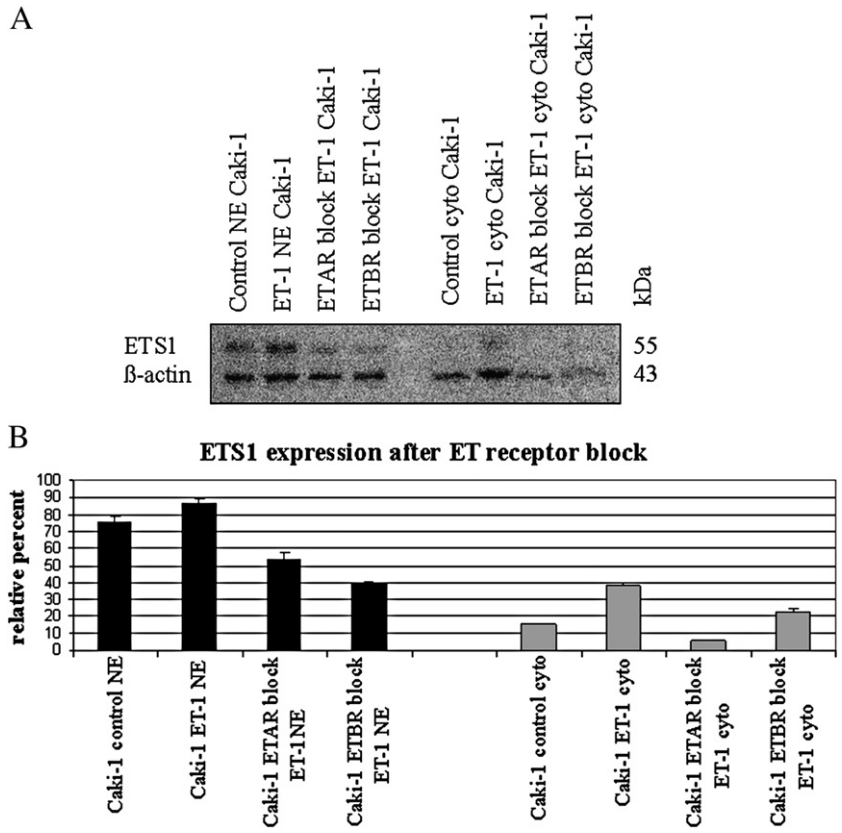

Fig. 3. In A, Western blot analysis of ETS1 protein levels after specific block of the endothelin receptors (n = 3) followed by ET-1 treatment. β-actin served as a loading control. In B, densitometric analysis of Western blot: results of the ANOVA with Bonferroni method indicated by stars.

statistical significance ($p<0.05$) for both experiments. An increase in signals per cell from 1.9 to 2.7 for ETS1 and ERK2 and an increase in signals per cell from 2.0 to 2.2 for the complex between ERK2 and Mxi2 after endothelin-1 treatment were detected. The quantification of fluorescent signals was done by using the Blobfinder program. The results confirm a complex formation between ETS1, ERK2 and Mxi2, already observed in immunoprecipitation. A location of the complex partners in the nucleus is seen, indicating a migration of the complex into the nucleus.

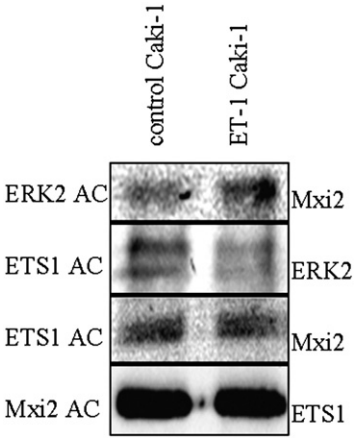

Fig. 4. Immunoprecipitation analysis of transcription complex. 1000 μg of total cell extracts from Caki-1 cells, stimulated with 50 nM ET-1 for 24 h was immunoprecipitated using agarose beads conjugated with antibodies against ERK2, ETS1, and Mxi2. After boiling and pelleting of the agarose beads, the supernatant was loaded onto an SDS-PAGE and blotted, and the associated proteins detected with specific antibodies. The experiments were performed in triplicate.

Cytoplasmic—nuclear transmigration

Immunoprecitation, in duplicate, of total cellular protein, isolated from 50 nM ET-1 stimulated cells for 24 h, was performed with ETS1 coated agarose beads. Following Western blot analysis, using antibodies against α and β-subunits of importins, we did not identify any importins involved in nuclear translocation (data not shown).

Endothelin receptor dependent $p16^{INK4a}$ expression and electrophoretic mobility shift assay analysis of binding partners in the transcription complex and their binding specificity

After treatment of the Caki-1 cells, $p16^{INK4a}$ PCR was performed and the PCR product was analyzed on a 2% agarose gel. Significantly decreased $p16^{INK4a}$ expression levels were detected after ETBR block.

By EMSA analysis, the binding of the ETS1-ERK2-Mxi2 transcription factor complex on the target gene $p16^{INK4a}$ was tested to investigate the activation of $p16^{INK4a}$ (Fig. 6B). Nuclear cell extracts from Caki-1 cells stimulated for 24 h with 50 nM ET-1 were incubated with oligonucleotides, representing the $p16^{INK4a}$ promoter sequence for ETS. A supershift analysis for ETS1 and Mxi2 was performed. The results show a shift for both, ETS1 and Mxi2, before and after ET-1 stimulation of the cells. The EMSAs were performed four times, always showing the same specificity. Samples incubated with oligonucleotides mutated in their consensus sequence, revealed a decrease in their fluorescent signal. A significant decrease of the $p16^{INK4a}$ signal was found in the case of Mxi2 supershift analysis. This indicates that

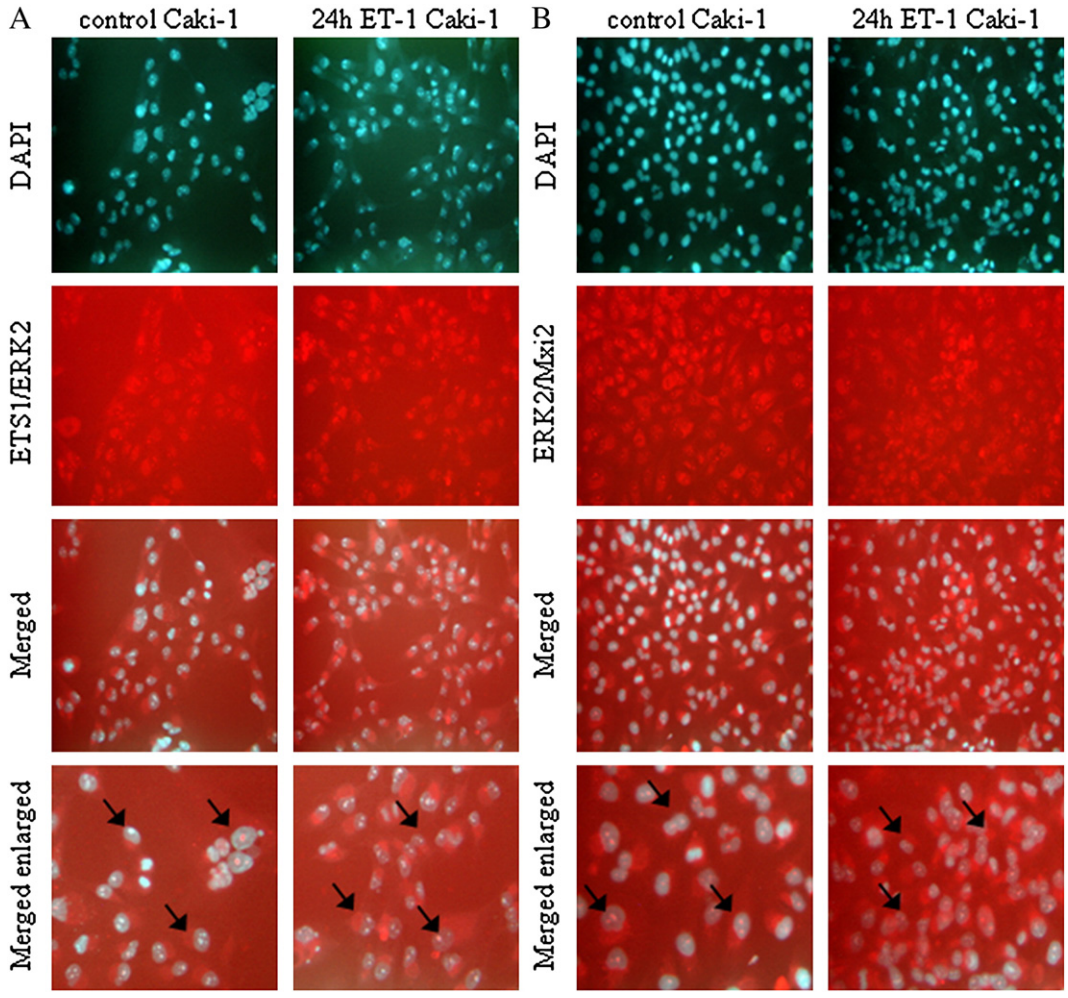

Fig. 5. Duolink in situ proximity ligation assay. 1×10^4 Caki-1 cells were grown on Labtecs, stimulated for 24 h with 50 nM ET-1 (n = 2). Protein complex formation was detected by specific antibodies coupled to oligonucleotides, which were detected after a ligation step with fluorescently labeled complementary oligonucleotides, leading to a nuclear, dot-like, fluorescent signal. Nuclear counterstain was performed using DAPI mounting medium (top row). In column A, the complex formation between ETS-1 with ERK-2 is shown with an increase in dots per cell from 1.9 to 2.7 after ET-1 stimulation. In column B, the complex formation between ERK-2 with Mxi-2 can be seen, with an increase in dots per cell after ET-1 stimulation from 2.0 to 2.2 The last row is an enlargement of row 3 (both columns), highlighting visible nuclear dot-like fluorescent signals (indicated by arrows).

the ETS1 binding site is essential for Mxi2 binding, since it is prevented by mutation analysis (Fig. 6B).

Comparison of ET-1 mediated ETS-1 induction in malignant Caki-1 versus primary RPTEC

As all experiments were performed in Caki-1 cells, the regulation of protein expression of ETS1 was tested in the non-malignant origin of Caki-1 cells, namely primary human RPTEC. Western blot analysis was carried out to show the protein expression of ETS1 in cytoplasmic and nuclear cell extracts (n = 3), after 50 nM ET-1 stimulation in both cell lines (Fig. 7). In Caki-1 cells, the amount of ETS1 was higher in the nucleus than in the cytoplasm with a significant increase after ET-1 stimulation. In contrast, in RPTEC the reverse could be seen: cytoplasmic content of ETS1 highly exceeded that of the nucleus. Furthermore, the amount of ETS1 dropped after ET-1 stimulation, while simultaneously being raised in the cytoplasm to the same amount (Fig. 7B).

Discussion

This study describes a cytoplasmic complex formation of three proteins: ETS1, ERK2, and Mxi2 after endothelin-1 stimulation, and their nuclear transmigration, leading to the upregulation of the tumor suppressor gene $p16^{INKa}$ (see Fig. 8) in malignant renal proximal tubule cells.

In renal clear cell carcinoma, the most prevalent of all encountered malignant, renal parenchymal tumors, the expression of the tumor suppressor gene $p16^{INK4a}$ has been described as downregulated. This was associated with a malignant phenotype as in other tumors. In contrast, the detection of $p16^{INK4a}$ expression in such tumors could be related to a tumor-specific improvement of patient survival (Ikuerowo et al., 2007). Thus, the analysis of transcription factors leading to its expression is helpful in understanding $p16^{INK4a}$ regulation and provides a basis for potential therapeutic approach. Since $p16^{INK4a}$ contains a promoter with an ETS factor specific binding site, we primarily analyzed the induction of ETS family members in the context of renal tumor cells after ET-1. The selection of specific members tested was based on previous work from Hollenhorst et al. (2004), showing that in renal tissue only a limited number of ETS family members were to be expected. Surprisingly, from those present only ETS1, ETS2 and GABPα showed significant upregulation after ET-1 stimulation (Fig. 1). Only ETS1 showed a highly statistically significant temporal regulation (Fig. 2A), with an increased presence in the nucleus at 24 h after ET-1. No increase of protein level was detectable in the nucleus for either ETS2 (Fig. 2B) or for GABPα (data not shown) Therefore, it is possible that the upregulated mRNA levels, detectable by PCR, undergo posttranscriptional modifications (Fig. 9).

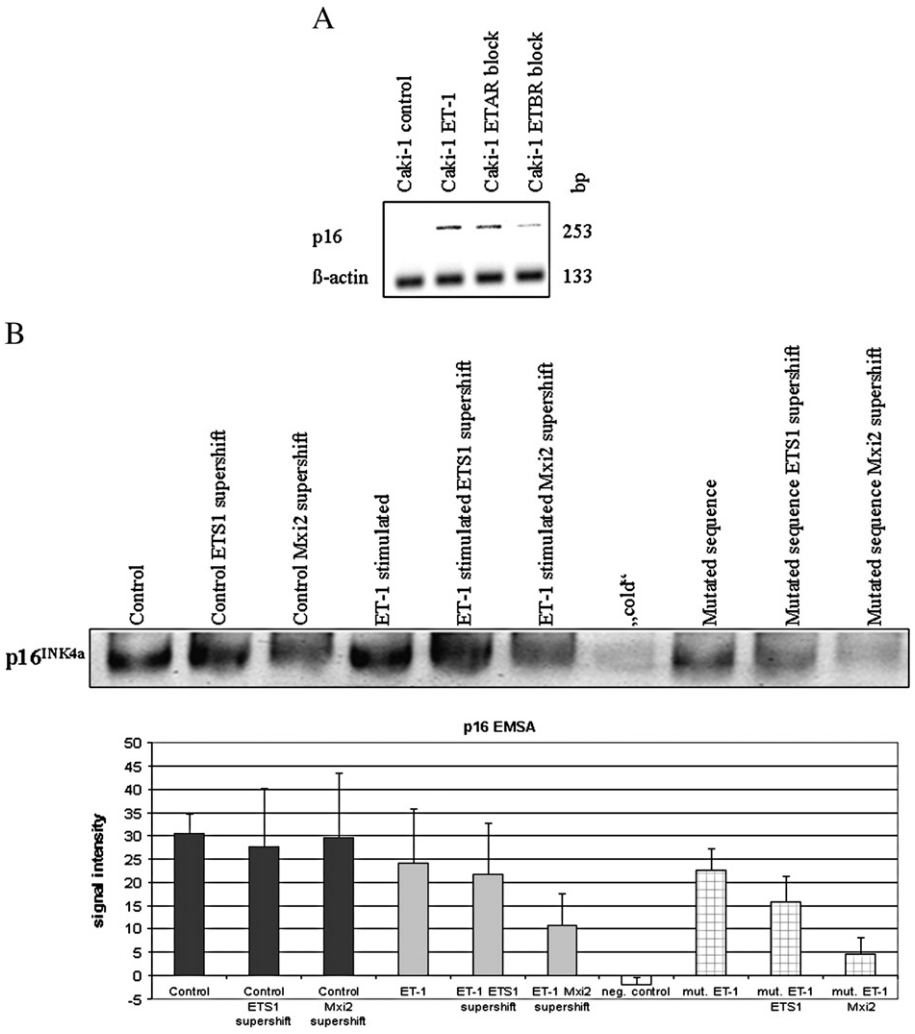

Fig. 6. In panel A, expression level of $p16^{INK4a}$ transcription factors in Caki-1 cells. Subconfluent cells were treated with a specific ETAR or ETBR blocker or/ and stimulated with 50 nM ET-1 for 24 h (after block). After RNA extraction, 250 ng was reverse transcribed, and a PCR reaction was performed using primers for ETS transcription factors. PCR products were analyzed on a 2% agarose gel (n = 2). In B, non-radioactive EMSA representing $p16^{INK4a}$ promoter sequence with supershift analysis for ETS1 and Mxi2. 20 μg nuclear extracts from Caki-1 cells were incubated with forward Alexa660 labeled oligonucleotides and reverse unlabeled oligonucleotides. For supershift analysis, ETS1 or Mxi2 antibody was pre-incubated for 1.5 h with the nuclear extract. Samples were loaded onto a 6% non-denaturing polyacrylamide gel and run at 100 V for 180 min. The EMSAs were performed four times, always showing the same specificity. For densitometric analysis shown in B, the signal intensity of the appropriated sample was calculated and the untreated Caki-1 cells were regarded as 100%.

Complex formation of ETS1 and other transcription factors, such as ERK2 (Seidel and Graves, 2002) is reported in literature, and ERK2 is known to form a complex with Mxi2 (Casar et al., 2007). Thus, it was tempting to investigate whether (i) these factors play a role in the setting of renal tumor signaling as well, and (ii) whether there might be a complex formation between all three factors as we described for MAPKp38, NF-κB p65 and PKCα after ET-1 stimulation in a variety of malignant tumor cells, including Caki-1 cells (von Brandenstein et al., 2008, 2011). In immunoprecipitation experiments with either ETS1, ERK2 or Mxi2 conjugated to agarose beads, interaction between the three proteins could be demonstrated (Fig. 4). Thus, a transcription complex consisting of all three proteins was detectable. Since, due to experimental restrictions, total cell extracts were used for this experiment, an independent method was employed to visualize the presence of this complex. In Caki-1 cells, the use of paired specific antibodies against either ETS1 and ERK2 (Fig. 5A) or ERK-2 and Mxi-2 (Fig. 5B) combined with oligonucleotide coupled secondary antibodies resulted in a nuclear fluorescent signal in the Duolink in situ proximity ligation assay, as predicted for complexes in which proteins involved are in close proximity (Fig. 5).

Nuclear transmigration may occur as a complex or by each protein individually. In analogy to our study showing the involvement of importins 4 and 5 as chaperone for the nuclear transmigration of the NF-κBp65/MAPK p38/PKCα complex (von Brandenstein et al., 2011), the potential involvement of the α-subunits and the β-subunit of importins was investigated by immunoprecipitation and subsequent Western blotting using specific antibodies (data not shown). However, no direct binding could be observed. Thus, we currently have to speculate whether or not the phosphorylated proteins may enter the nucleus by active transport (Formstecher et al., 2001; Whitehurst et al., 2004) individually, such as it was suggested for ERK1/2 after phosphorylation (Lenormand et al., 1993). Alternatively, it has been speculated that Mxi2 itself may serve as a chaperone protein (Casar et al., 2007). Finally, importin 8, which is a protein binding to the nuclear pore complex, and shares a sequence motif related to the Ran-binding site of importin β (Weinmann et al., 2009), could also serve as a potential chaperone.

$p16^{INK4a}$ has a known binding site for ETS proteins in its promoter, raising the question of whether ETS1 after nuclear transmigration would bind as an individual protein or whether the entire newly

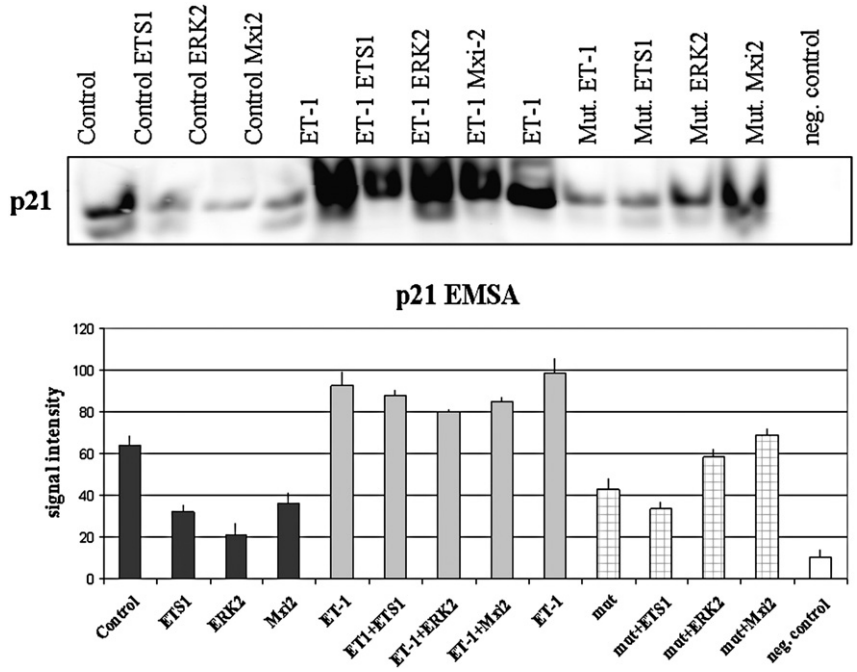

Fig. 7. Non-radioactive EMSA representing p21$^{waf1/cip1}$ promoter sequence with supershift analysis for ETS1 and Mxi2. 20 μg nuclear extracts from Caki-1 cells were incubated with forward Alexa660 labeled oligonucleotides and reverse unlabeled oligonucleotides. For supershift analysis, ETS1 or Mxi2 antibody was pre-incubated for 1.5 h with the nuclear extract. Samples were loaded onto a 6% non-denaturing polyacrylamide gel and run at 100 V for 120 min. The EMSAs were performed four times, always showing the same specificity. For densitometric analysis shown in B, the signal intensity of the appropriated sample was calculated and the untreated Caki-1 cells were regarded as 100%.

identified transcription factor complex was part of the p16^{INK4a} transcription machinery. An EMSA with subsequent supershift analysis for ETS1 and Mxi2 reveals that both proteins bind as a complex to the p16^{INK4a} promoter in Caki-1 cells (Fig. 6B). The specificity of this binding can be demonstrated by mutating the ETS binding of the p16^{INK4a} promoter with a significant loss of activity. In addition, the importance of the flanking sequence of the ETS-binding site is shown by a dramatic loss of signal intensity. A significant decrease of the p16^{INK4a} signal was found in case of Mxi2 supershift analysis, indicating that the ETS1 binding site is essential for Mxi2 binding as shown by mutation analysis (Fig. 6B).

We also investigated the question which of the two endothelin receptors is important for p16^{INK4a} production. After specific block of the two receptors, followed by ET-1 treatment, the mRNA expression was analyzed. As it can be seen in Fig. 6A, both blocking experiments lead to a reduction of the p16^{INK4a} expression level, however, the ETBR block was more significant. This result correlates with our previously findings where both receptor blocks lead to a reduction of the protein level of ETS1. In this case, the ETBR block was also more significant and resulted in a decrease of ETS1 protein levels in the

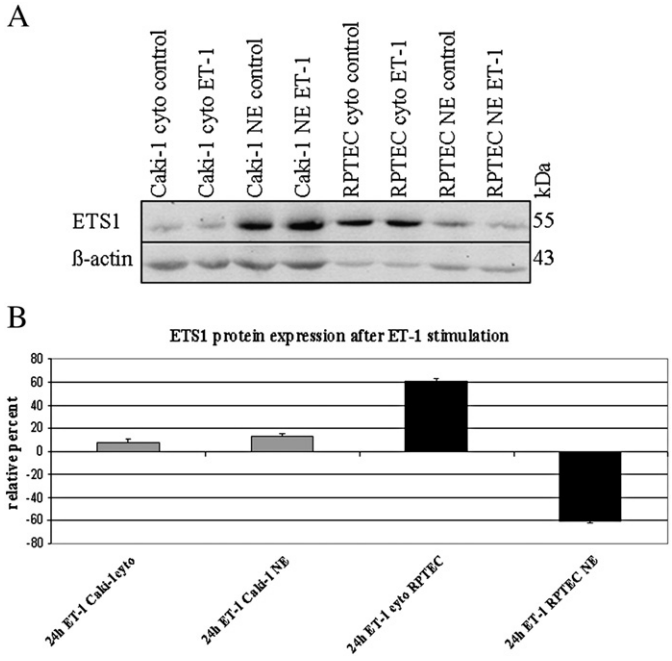

Fig. 8. Nuclear and cytoplasmic ETS1 protein expression in Caki-1 versus primary human proximal tubule epithelial cells (RPTEC). Western blots were performed in triplicate. In panel A, Western blot analysis of cytoplasmic and nuclear extracts from Caki-1 versus RPTEC cells stimulated with 50 nM ET-1 for 24 h were analyzed with an ETS1 antibody. β-actin served as a loading control. In panel B, densitometric analysis of performed Western blots.

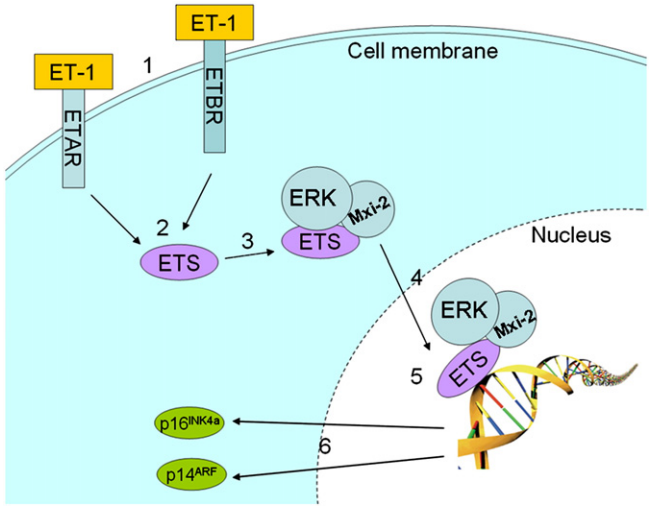

Fig. 9. Schematic presentation of the signaling cascade connecting ET-1 stimulation to p16^{INK4a} activation in Caki-1 cells according to the results of this study. After ET-1 stimulation ETS1 forms a complex with ERK2 and Mxi2, which is translocated into the nucleus, where the complex binds via ETS1 to the ETS-binding site in the p16^{INK4a} promoter, initiating p16^{INK4a} gene expression.

nucleus of Caki-1 cells (Fig. 4A). Due to the fact that ETS1 can bind to the $p16^{INK4a}$ promoter region shown by EMSA (Fig. 6B) and leading therefore to an activation of $p16^{INK4a}$ expression, a decrease of ETS1 after ETBR block leads to a reduction of $p16^{INK4a}$ levels. This result differs from the one reported by Terada et al. (1998) who found that the $p16^{INK4a}$ activation is endothelin A receptor dependent. Furthermore, ET-1 stimulated [^{3}H] thymidine incorporation, CDK4 kinase activity, and prevention of cells in S phases were significantly inhibited by the overexpression of $p16^{INK4a}$ and slightly inhibited by the overexpression of $p21^{waf1/cip1}$. This result seems puzzling, since others have reported the involvement of the ETB receptor as mediator of ET-1 stimulation in mesangial proliferative glomerulonpehritis in the rat (Yoshimura et al., 1995). Here, the model system used (cell culture versus animal model) as well as additional unknown factors co-activated by ET1 stimulation may play a yet important but undiscovered role. This difference between our observation and Terada et al. (1998) may be explained in part by the use of different cell types (mesangial vs tubular epithelial cells) as well as the use of different species (rat versus human), since the signaling loop seems to be species as well as cell type specific (Gerstung et al., 2007).

$p21^{waf1/cip1}$ has a functional binding site for ETS proteins in its promoter (Zhang et al., 2003), raising the question of whether ETS1 after nuclear transmigration would bind as an individual protein or whether the entire newly identified transcription factor complex was also part of the $p21^{waf1/cip1}$ transcription machinery. An EMSA with subsequent supershift analysis for ETS1, ERK2 and Mxi2 reveals that both proteins bind as a complex to the $p21^{waf1/cip1}$ promoter in Caki-1 cells (Fig. 7). The specificity of this binding can be demonstrated by mutating the ETS binding of the $p21^{waf1/cip1}$ promoter with a significant loss of activity.

Caki-1 cells are the malignant counterpart of proximal renal tubule cells. In those tubule cells, protein loss through the glomerular basement membrane in a variety of immunologic and non-immunologic diseases has been identified as an important pathophysiologic mechanism for $p16^{INK4a}$ upregulation (Sis et al., 2007) In the context of proteinuric stimulation, ET-1 seems to be a major stimulus for proximal tubule activation (Abbate et al., 2006; Zoja et al., 2003). The current notion is that tubular injury may exhaust finite replicative capacity. This could be detrimental to renal function, since it leads to progressive nephron loss with replacement fibrosis, ultimately causing chronic renal insufficiency and necessitating dialysis (Meyer, 2003). Because ETS1 binding via its specific binding site to the $p16^{INK4a}$ promoter can be considered essential for $p16^{INK4a}$ transcription, we investigated the cytoplasmic and nuclear temporal expression profile of ETS1 in human primary renal proximal tubule cells (RPTEC). Pathophysiological activation was mimicked by adding ET-1 to the culture medium for 24 h. The result in Fig. 8 shows that the majority of ETS1 expression is located in the cytoplasm and only about one-fourth of detectable protein is found in the nucleus in RPTECs. Unexpectedly, this result changes after ET-1 stimulation opposite to that observed in malignant Caki-1 cells, i.e., the amount of ETS1 decreases in the nucleus, and the decreased amount seems to be added to the amount of detectable protein in the cytoplasm, presumably by nuclear export. This result is in contrast to the observed increase in $p16^{INK4a}$ immunostaining in proximal tubules in proteinuric conditions (Sis et al., 2007), indicating that under proteinuric conditions in normal proximal tubule cells other members of the ETS family may be responsible for $p16^{INK4a}$ binding and thus necessitating further studies.

Conclusion

In conclusion, we demonstrate that in renal carcinoma a transcription complex, consisting of: ETS1, ERK2 and Mxi2 is responsible for increased $p16^{INK4a}$ protein expression, leading to an improved disease survival, according to the literature. Furthermore, it was also possible to show that the $p16^{INK4a}$ expression is ETBR > ETAR dependent.

In this context, ET-1 is a helpful adjunct by further promoting $p16^{INK4a}$ expression. Since ETS1 is decreased in the nuclei of normal proximal kidney cells after ET-1 stimulation potentially observed in proteinuria, other members of the ETS transcription family may be responsible for the observed $p16^{INK4a}$ overexpression under these circumstances.

Author's contribution

MvB: cell culture, proximity ligation assay, Western blot, EMSA. MS: cell culture, Western blot, EMSA, qRT-PCR, PCR, immunoprecipitation. CR: RNA isolation, cell culture. RD: chaperone testing. JWUF: experimental design, writing of manuscript. MvB, MS, JWUF: interpretation of study, and discussion of experimental results. All authors drafted, read and approved the manuscript.

Conflict of interest statement

No conflict declared.

Acknowledgements

The study was supported by the Koeln Fortune Program / Faculty of Medicine, University of Cologne post-doctoral fellowship and a grant from the 2nd Professorinnen Program (to MvB); by a grant from the Marga and Walter Boll Stiftung, Imhoff Stiftung, and the Nolting Stiftung (to JWUF). Since human cells were used, procedures have been followed as outlined in accordance with ethical standards as formulated in the Helsinki Declaration of 1975 (revised 1983). The use of patient tumor samples was approved by the University of Koeln Research Ethics Committee.

References

Abbate M, Zoja C, Remuzzi G. How does proteinuria cause progressive renal damage? J Am Soc Nephrol 2006;17:2974–84.
Casar B, Sanz-Moreno V, Yazicioglu MN, Rodriguez J, Berciano MT, Lafarga M, et al. Mxi2 promotes stimulus-independent ERK nuclear translocation. EMBO J 2007;26:635–46.
Chen QW, Edvinsson L, Xu CB. Role of ERK/MAPK in endothelin receptor signaling in human aortic smooth muscle cells. BMC Cell Biol 2009;10:52.
Faccio L, Chen A, Fusco C, Martinotti S, Bonventre JV, Zervos AS. Mxi2, a splice variant of p38 stress-activated kinase, is a distal nephron protein regulated with kidney ischemia. Am J Physiol Cell Physiol 2000;278:C781–90.
Formstecher E, Ramos JW, Fauquet M, Calderwood DA, Hsieh JC, Canton B, et al. PEA-15 mediates cytoplasmic sequestration of ERK MAP kinase. Dev Cell 2001;1:239–50.
Franco OE, Onishi T, Umeda Y, Soga N, Wakita T, Arima K, et al. Phenylacetate inhibits growth and modulates cell cycle gene expression in renal cancer cell lines. Anticancer Res 2003;23:1637–42.
Gerstung M, Roth T, Dienes HP, Licht C, Fries JW. Endothelin-1 induces NF-kappaB via two independent pathways in human renal tubular epithelial cells. Am J Nephrol 2007;27:294–300.
Gutierrez-Hartmann A, Duval DL, Bradford AP. ETS transcription factors in endocrine systems. Trends Endocrinol Metab 2007;18:150–8.
Hollenhorst PC, Jones DA, Graves BJ. Expression profiles frame the promoter specificity dilemma of the ETS family of transcription factors. Nucleic Acids Res 2004;32:5693–702.
Hui R, Macmillan RD, Kenny FS, Musgrove EA, Blamey RW, Nicholson RI, et al. INK4a gene expression and methylation in primary breast cancer: overexpression of p16INK4a messenger RNA is a marker of poor prognosis. Clin Cancer Res 2000;6:2777–87.
Ikuerowo SO, Kuczyk MA, von Wasielewski R, Shittu OB, Jonas U, Machtens S, et al. p16INK4a expression and clinicopathologic parameters in renal cell carcinoma. Eur Urol 2007;51:732–7. [discussion 8].
Jedlicka P, Gutierrez-Hartmann A. Ets transcription factors in intestinal morphogenesis, homeostasis and disease. Histol Histopathol 2008;23:1417–24.
Jung YS, Qian Y, Chen X. Examination of the expanding pathways for the regulation of p21 expression and activity. Cell Signal 2010;22:1003–12.
Krimpenfort P, Quon KC, Mooi WJ, Loonstra A, Berns A. Loss of p16Ink4a confers susceptibility to metastatic melanoma in mice. Nature 2001;413:83–6.
Lenormand P, Sardet C, Pages G, L'Allemain G, Brunet A, Pouyssegur J. Growth factors induce nuclear translocation of MAP kinases (p42mapk and p44mapk) but not of their activator MAP kinase kinase (p45mapkk) in fibroblasts. J Cell Biol 1993;122:1079–88.

Lin AW, Barradas M, Stone JC, van Aelst L, Serrano M, Lowe SW. Premature senescence involving p53 and p16 is activated in response to constitutive MEK/MAPK mitogenic signaling. Genes Dev 1998;12:3008–19.
Maruschke M, Thur S, Kundt G, Nizze H, Hakenberg OW. Immunohistochemical expression of retinoblastoma protein and p16 in renal cell carcinoma. Urol Int 2011;86:60–7.
Meyer TW. Tubular injury in glomerular disease. Kidney Int 2003;63:774–87.
Ohtani N, Zebedee Z, Huot TJ, Stinson JA, Sugimoto M, Ohashi Y, et al. Opposing effects of Ets and Id proteins on p16INK4a expression during cellular senescence. Nature 2001;409:1067–70.
Ong AC, Jowett TP, Firth JD, Burton S, Karet FE, Fine LG. An endothelin-1 mediated autocrine growth loop involved in human renal tubular regeneration. Kidney Int 1995;48:390–401.
Ortmann J, Amann K, Brandes RP, Kretzler M, Munter K, Parekh N, et al. Role of podocytes for reversal of glomerulosclerosis and proteinuria in the aging kidney after endothelin inhibition. Hypertension 2004;44:974–81.
Park WH, Jung CW, Park JO, Kim K, Kim WS, Im YH, et al. Monensin inhibits the growth of renal cell carcinoma cells via cell cycle arrest or apoptosis. Int J Oncol 2003;22:855–60.
Puri S, Rodova M, Islam MR, Magenheimer BS, Maser RL, Calvet JP. Ets factors regulate the polycystic kidney disease-1 promoter. Biochem Biophys Res Commun 2006;342:1005–13.
Sanz-Moreno V, Casar B, Crespo P. p38alpha isoform Mxi2 binds to extracellular signal-regulated kinase 1 and 2 mitogen-activated protein kinase and regulates its nuclear activity by sustaining its phosphorylation levels. Mol Cell Biol 2003;23:3079–90.
Seidel JJ, Graves BJ. An ERK2 docking site in the Pointed domain distinguishes a subset of ETS transcription factors. Genes Dev 2002;16:127–37.
Sis B, Tasanarong A, Khoshjou F, Dadras F, Solez K, Halloran PF. Accelerated expression of senescence associated cell cycle inhibitor p16INK4A in kidneys with glomerular disease. Kidney Int 2007;71:218–26.
Terada Y, Inoshita S, Nakashima O, Yamada T, Tamamori M, Ito H, et al. Cyclin D1, p16, and retinoblastoma gene regulate mitogenic signaling of endothelin in rat mesangial cells. Kidney Int 1998;53:76–83.
Verzola D, Gandolfo MT, Gaetani G, Ferraris A, Mangerini R, Ferrario F, et al. Accelerated senescence in the kidneys of patients with type 2 diabetic nephropathy. Am J Physiol Renal Physiol 2008;295:F1563–73.
von Brandenstein MG, Ngum Abety A, Depping R, Roth T, Koehler M, Dienes HP, et al. A p38-p65 transcription complex induced by endothelin-1 mediates signal transduction in cancer cells. Biochim Biophys Acta 2008;1783:1613–22.
von Brandenstein M, Depping R, Schafer E, Dienes HP, Fries JW. Protein kinase C alpha regulates nuclear pri-microRNA 15a release as part of endothelin signaling. Biochim Biophys Acta 2011;1813:1793–802.
Weinmann L, Hock J, Ivacevic T, Ohrt T, Mutze J, Schwille P, et al. Importin 8 is a gene silencing factor that targets argonaute proteins to distinct mRNAs. Cell 2009;136:496–507.
Whitehurst AW, Robinson FL, Moore MS, Cobb MH. The death effector domain protein PEA-15 prevents nuclear entry of ERK2 by inhibiting required interactions. J Biol Chem 2004;279:12840–7.
Yoshimura A, Iwasaki S, Inui K, Ideura T, Koshikawa S, Yanagisawa M, et al. Endothelin-1 and endothelin B type receptor are induced in mesangial proliferative nephritis in the rat. Kidney Int 1995;48:1290–7.
Yu SJ, Kim HS, Cho SW, Sohn J. IL-4 inhibits proliferation of renal carcinoma cells by increasing the expression of p21WAF1 and IRF-1. Exp Mol Med 2004;36:372–9.
Zervos AS, Faccio L, Gatto JP, Kyriakis JM, Brent R. Mxi2, a mitogen-activated protein kinase that recognizes and phosphorylates Max protein. Proc Natl Acad Sci U S A 1995;92:10531–4.
Zhang C, Kavurma MM, Lai A, Khachigian LM. Ets-1 protects vascular smooth muscle cells from undergoing apoptosis by activating p21WAF1/Cip1: ETS-1 regulates basal and inducible p21WAF1/Cip: ETS-1 regulates basal and inducible p21waf1/cip1 transcription via distinct cis-acting elements in the p21WAF/Cip1 promoter. J Biol Chem 2003;278:27903–9.
Zoja C, Morigi M, Remuzzi G. Proteinuria and phenotypic change of proximal tubular cells. J Am Soc Nephrol 2003;14(Suppl. 1):S36–41.